ADVANCED FUNCTIONAL MATERIALS

FULL PAPER

Spatially Selective Nucleation of Metal Clusters on the Tobacco Mosaic Virus

By *Mato Knez*, *Martin Sumser*, *Alexander M. Bittner*,* *Christina Wege*, *Holger Jeske*, *T. Patrick Martin*, and *Klaus Kern*

Tobacco mosaic virus (TMV) is a very stable nanotube complex of a helical RNA and 2130 coat proteins. The special shape makes it an interesting nano-object, especially as a template for chemical reactions. Here we use TMV as a chemically functionalized template for binding metal ions. Different chemical groups of the coat protein can be used as ligands or to electrostatically bind metal ions. Following this activation step, chemical reduction and electroless plating produces metal clusters of several nanometers in diameter. The clusters are attached to the virion without destroying its structure. Gold clusters generated from an ascorbic acid bath bind to the exterior surface as well as to the central channel of the hollow tube. Very high selectivity is reached by tuning Pd^{II} and Pt^{II} activations with phosphate: When TMV is first activated with Pd^{II}, and thereafter metallized with a nickel–phosphinate bath, 3 nm nickel clusters grow in the central channel; when TMV from phosphate-buffered suspensions is employed, larger nickel clusters grow on the exterior surface. Phosphate buffers have to be avoided when 3 nm nickel and cobalt wires of several 100 nm in length are synthesized from borane-based baths inside the TMV channel. The results are discussed with respect to the inorganic complex chemistry of precursor molecules and the distribution of binding sites in TMV.

1. Introduction

The fabrication of nanostructures with well-defined chemical composition and low defect concentration is a prerequisite for the determination of their intrinsic physical properties. The chemical composition is usually as simple as possible, i.e., elementary or binary. However, nanostructures are usually much larger than molecules and they do show defects and thus non-uniformity. Chemically speaking, a macroscopic sample of nano-objects consists of a distribution of different molecular species. The "size gap" between small molecules and nano-objects is currently being filled with interesting larger tailor-made molecules,[1] clusters of narrow size distributions,[2,3] and supramolecules.[1,4,5] Directly connected to the size is the problem of uniform chemical composition. While in a large cluster the exact number of atoms is usually not important, the chemical nature—especially when the exterior elemental composition is different from the interior one—can significantly alter the properties.[3] On the other hand, the exact number of such heteroatoms is extremely difficult to control. This "chemistry gap" also becomes evident for very large molecular entities with a certain number of functional groups. The best examples are probably proteins where a single amino acid change can render the molecule functional or non-functional (see Wilson and Perham[6] for chemical modifications and Stubbs[7] and Demir and Stowell[8] for examples of site-directed mutagenesis, both of the coat protein of the tobacco mosaic virus). This leads to the idea of using biomolecules either as functional nanostructures or as templates for such. Plant viruses are especially suitable, as exemplified by the synthesis of tungstate and vanadate inside the cowpea chlorotic mottle virus[9] by pH-controlled opening and closing of the icosahedral virion cage. Recently, Wang et al.[10] modified cowpea mosaic viruses genetically to display sulfhydryl groups on their exterior surface. Gold nanoclusters were selectively attached to these moieties in icosahedral symmetry, reflecting the virion symmetry.

In order to have a large number of chemical functions but a well-defined and even stable structure we chose tobacco mosaic virus (TMV), a hollow tube compound (see Fig. 1) that comprises a helical RNA strand and 2130 coat proteins. The proteins are helically arranged with 16.3 units building up one turn. The particle length is 300 nm with 18 nm exterior and 4 nm inner diameter[7,11,12] (the RNA helix has an 8 nm diameter). The special shape makes this virus an interesting nano-object, especially as a template, demonstrated by the crystallization of inorganic materials on TMV[13] and by the attachment of metal clusters to its surfaces.[8,14–17] Continuous coating of the outer virion surface with metal could not be effected, although nanowires can be synthesized in the inner channel.[18] The advantage of TMV is that temperatures of up to 90 °C and pH values from 3.5 up to approximately 9 do not affect the

[*] Dr. A. M. Bittner, M. Knez, Dr. T. P. Martin, Prof. K. Kern
Max-Planck-Institut für Festkörperforschung
Heisenbergstr. 1, D-70569 Stuttgart (Germany)
E-mail: a.bittner@fkf.mpg.de
M. Sumser, Dr. C. Wege, Prof. H. Jeske
Biologisches Institut
Department of Molecular Biology and Plant Virology
Universität Stuttgart
Pfaffenwaldring 57, D-70550 Stuttgart (Germany)

[**] We thank M. Kelsch and Dr. F. Phillipp (Max-Planck-Institut für Metallforschung, Stuttgart) for their valuable help with transmission electron microscopy. We thank F. Boes and A. Kadri (Universität Stuttgart) and Prof. Dr. E. Maiß (Universität Hannover) for their help with producing Ser155-replaced TMV. We gratefully acknowledge discussions with Prof. Dr. K.-W. Mundry.

  DOI: 10.1002/adfm.200304376

ADVANCED FUNCTIONAL MATERIALS

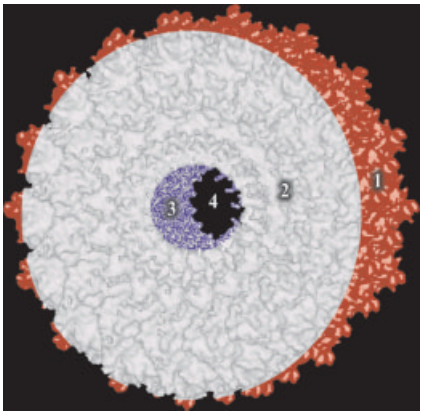

Figure 1. Sketch of the TMV (ca. 7 nm of 300 nm length are shown). The exterior surface, (1), is composed of the amino acids of the coat protein, which are located near the amine and carboxylate termini. (2) is the densely packed bulk of the coat protein. (3) denotes the surface of the central channel, composed of amino acid loops. (4) is the hollow part of the central channel, usually filled with water.

structure over a period of hours,[19] and that it remains intact even in organic solvents such as ethanol or in aqueous dimethylsulfoxide (DMSO). The coat protein contains no His, and no Met, and only a single Cys. The exterior surface provides functional groups including serine and threonine (OH groups) as well as the COOH terminus of the coat protein. More groups become accessible when the outermost part of the coat protein changes its conformation. The central channel is similarly composed, but also exhibits some primary amide groups[11] and shows less conformational stability. This chemical versatility on the nanometer scale might be an advantage in comparison to other nano-objects such as chemically uniform carbon nanotubes or inorganic nanowires. Recently,[20] we found that the adsorption properties depend strongly on the chemical properties of the terminal COOH groups and on the OH functions. This can be exploited by tuning the pH value of a TMV suspension to fit the substrate chemistry. Even covalent linkages from surfaces to these groups are possible.[20]

Here we show how the chemical versatility of the virion can be used for spatially selective metallizations. We produced metal clusters on the nanometer length scale that were firmly attached to the virion, without destroying its geometry. To obtain a strong bond, we produced the clusters by firstly binding the pertaining ions to TMV and subsequently reducing them. This process was—in the case of palladium, platinum, and gold—followed by an electroless deposition of another metal from a bath. The latter method turned out to be especially mild. The same strategy has recently been employed to metallize other biomaterials like DNA,[21,22] protein tubes,[23,24] protein fibers,[25] and also to fabricate metallic nanotubes in track etch membranes.[26] We show that the spatially selective metallization of the exterior surface and/or of the central channel of TMV is possible, while immuno-gold labeling[14] and crystallizations[13] are confined to the exterior surface.

2. Results and Discussion

2.1. Binding of UO_2^{2+} and Ru^{III} (Staining)

The standard technique for visualization of small biological structures is "negative staining" with a solution of $UO_2(CH_3COO)_2$. The compound precipitates at the surfaces of biomaterials without selectivity. For TMV, the exterior coat protein surface of the viral rod, as well as the central channel, were stained (Fig. 2). The staining mechanism implies that single ions are not adsorbed, but rather an—albeit very thin—layer of uranyl acetate. The short distance between the dark lines in

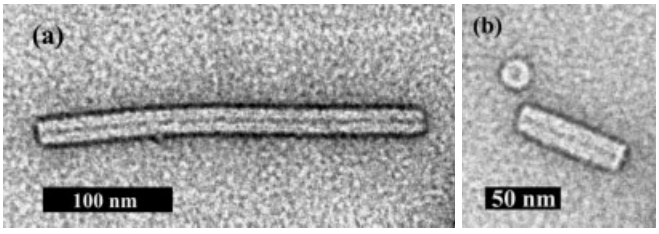

Figure 2. Transmission electron microscopy (TEM) images of TMV at 400 kV. a) Intact virion, 300 nm in length, 18 nm in width, stained with uranyl acetate. The central channel and the exterior surface appear black, i.e. uranium-rich. b) Virion fragment, ca. 80 nm in length, 18 nm in width; in the upper left part a disc is visible: A very short fragment adsorbed in vertical orientation (channel pointing in the direction of the view axis), thus the channel appears as small dark disc inside the larger one. In both images, the separation of the dark lines (i.e. the width of the bright part) is ca. 18 nm, while the distance between the outer borders of the dark lines is ca. 23 nm.

Figure 2 confirms this picture: This distance is in perfect agreement with the 18 nm outer diameter of the virion, hence uranyl is attached to the exterior surface of the virion, indicating an exclusive negative staining. We can expect a more ion-pair-like binding of this layer to the charged surfaces of the inner channel and of the outer viral surface (surfaces 3,1 in Fig. 1). Figure 2 shows that, while these parts are stained, the inside of the coat protein (structure 2 in Fig. 1) remains unstained (bright), hence uranyl cations do not penetrate into a protein. The high mass of U^{VI} translates into a high electron density and thus into a gray or black color on transmission electron microscopy (TEM) images. In principle, the very fine distribution of the uranium would be attractive for further metallization; however, extremely strong reductants would be necessary to reach the zero valent state (stable below –1.8 V_{SHE} (SHE = standard hydrogen electrode));[27] these would very likely lead to destruction of the biomaterial. On the other hand, the staining of a virion after a metallization would interfere with the deposited metals/metal ions, so we did not employ this method further. For direct comparison with the metallization experiments we recorded TEM images without staining (Fig. 3).

Staining of TMV can also be accomplished with Ru^{III}, which we discovered when we checked for possible ruthenium deposi-

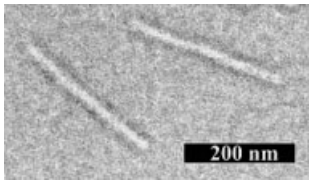

Figure 3. TEM image of unstained TMV (200 kV). There are no parts that are much darker than the background, but the inner part appears white and the exterior gray. The contrast was not enhanced by any staining. The bright inner part of the virion has a width of ca. 14 nm, while the distance between the outer borders (darker lines) is ca. 18 nm.

tion. Note that a reduction of Ru^{III} to Ru^{II} can be achieved only with very strong reductants, e.g., with Ti^{3+}, although this still does not yield metallic ruthenium.[28] Electroless deposition of ruthenium is reported in the literature,[29,30] but only at slightly harsher conditions than allowed for TMV, i.e., around pH 9 and temperatures around 90 °C. Since those conditions would destroy the viral integrity, lower temperatures (75 °C) and lower basicity (pH 8) were used. The TEM image (Fig. 4) shows only shading around the outer viral surface and inside the channel, comparable to the case of uranyl staining. No discrete clusters of metal could be observed. Pre-treatment of TMV with palladium and platinum before ruthenium deposition was tried, but yielded identical results. Similar to the case of uranyl, the shortest distance between the dark lines (Fig. 4) is ca. 18 nm, hence again a negative staining was achieved. The silver procedure we employed before[15] is also reminiscent of negative staining, but larger metallic clusters were produced.

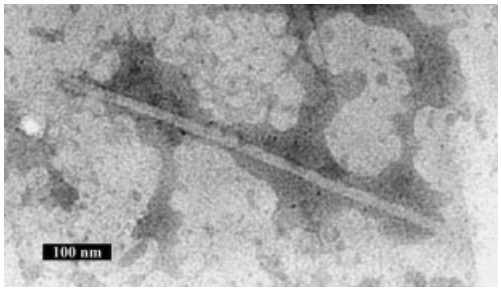

Figure 4. TEM image (200 kV) of two linearly arranged TMV after treatment with Ru^{III}. The outer borders of the virions as well as the inner channel appear dark, which is due to staining of the TMV with Ru^{III}. The width of the bright part is ca. 18 nm.

2.2. Reduction of Pd^{II} Bound to the Exterior Surface

When a TMV suspension is treated with $PdCl_4^{2-}$, hydrolysis of the palladate has to be prevented,[31] otherwise polyoxo-hydroxo-palladate nodules would form. These can easily reach several 100 nm in diameter (while clusters of less than 4 nm diameter are wanted). Suppression of this effect is afforded by a high Cl^- concentration, a low pH, and by working quickly, since the hydrolysis requires minutes to hours. TMV can then be recovered after centrifugation and washing. To prevent hydrolysis and dissociation of bound Pd^{II}, washing with a low-pH, high chloride concentration solution may be preferable to pure water. Pd^{II} was unable to stain the TMV, presumably because only a small amount was bound. If a reducing agent, e.g., hypophosphite, was added to the Pd^{II}-containing solution, a coverage of the exterior surface of the TMV with palladium was effected. Figure 5 shows two head-to-tail arranged TMVs, densely covered with palladium particles (comparable to the gold cluster decoration in ref.[16]).

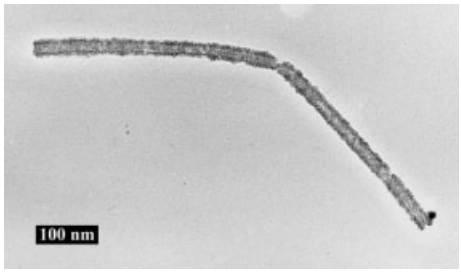

Figure 5. TEM (200 kV) of two TMVs, densely covered with palladium particles after treatment of the TMV with a hypophosphite-containing Pd^{II} solution.

The Pd^{II} complex $[PdCl_4]^{2-}$ is negatively charged and thus can be attracted by the positively charged outer surface of the virion at pH 5–6. [16] The surface of the inner channel is, in this pH regime, predominantly negatively charged, acting repulsively on the Pd^{II} complex. The result is an attachment of Pd^{II} exclusively to the outer surface and thus, upon reduction to palladium, metallic clusters positioned at the outer surface. During or after reduction, the metal atoms coalesce to clusters (see also refs.[8,16]). In contrast to the binding of the metal ions, the binding of the clusters to the virion relies on unknown factors—the bond between metal atoms and typical ligand groups, including RNA and coat protein, is usually too weak to account for it, and indeed the clusters may be mobile. Kind et al.[31] discussed the case of mobile palladium islands on an organic self-assembled monolayer with a terminal amine group, which might be comparable with small metal clusters on the exterior viral surface (surface 1 in Fig. 1), or even on the channel walls (surface 3 in Fig. 1).

2.3. Electroless Deposition of Nickel and Cobalt on the Exterior Surface

After a Pd^{II} or Pt^{II} activation (see Experimental), TMV was placed in a nickel or cobalt electroless deposition bath. Depending on the chemistry, it was adjusted to a specially selected pH (range 6–9) and in some cases heated to 50 °C. Conditions of < pH 6 or T < 20 °C decreased the deposition rate or even stopped the process. pH values above 9 destroyed the virions, whereas higher temperatures (> 70 °C) made the deposition un-

ADVANCED FUNCTIONAL MATERIALS

controllably fast. Deposition of nickel and cobalt without Pd^{II}—or Pt^{II}—pre-treatment of TMV was impossible.

A metallization with dimethylamine-borane (DMAB)-containing nickel (pH 6–7) or cobalt (pH 7–8) baths[23] was applied to undialyzed virions, i.e., the virus suspension contained small amounts of phosphate (which could not act as buffer due to their very low concentrations). The deposition rate increased strongly with temperature; at > 85 °C the reaction became uncontrollable. At 25 °C, metal deposition was restricted to the exterior surface of the virion (see Fig. 6). The deposition rate in nickel and cobalt reactions was slightly higher than in the reactions with dialyzed virions (described in Sec. 4).

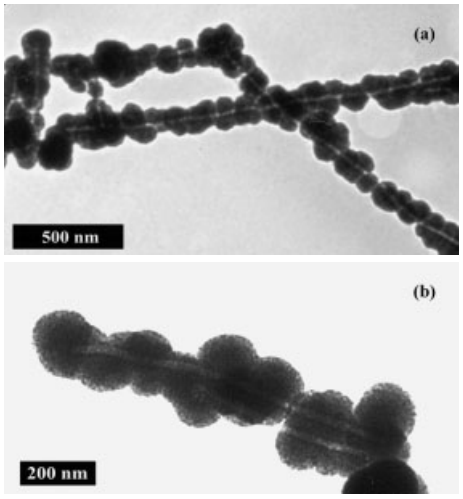

Figure 6. TEM (200 kV) micrographs of undialyzed and Pt^{II}-pre-treated TMV, metallized with nickel from a DMAB-containing nickel bath (a), and with cobalt from a DMAB-containing cobalt bath (b).

DMAB will first reduce Pd^{II} or Pt^{II} and produce small clusters (see Sec. 2). Hence the observed large clusters (> 50 nm diameter) contain nickel (or cobalt) and less than 1 % palladium or platinum. Their nearly spherical shape results from the fast plating of a few nuclei that then coalesced. The fact that no smooth cylinder is found means that the activation was not ideal, i.e., the coverage with palladium or platinum nuclei was too small. The selectivity for the exterior surface (1 in Fig. 1) is caused by phosphate ions that can bind electrostatically—in this pH region—to the positively charged exterior surface. A treatment with the Pd^{II} solution should yield co-existent Pd^{II} complexes (electrostatically bound, see also Sec. 4) and phosphate ions at the exterior surface of the virion. It is unlikely that Pd^{II} forms complexes with phosphate, since the few known complexes of this kind are either synthesized in absence of water at temperatures higher than 230 °C or photochemically. However, Co^{II} and Ni^{II} precipitate easily with phosphate, presumably in the form $Ni_3(PO_4)_2{\cdot}xH_2O$ or $Co_3(PO_4)_2{\cdot}xH_2O$. Upon contact with the phosphate-covered virions, Ni^{II} or Co^{II} precipitate in this form on the exterior virion surface. The reduction to metal requires Pd^{II}, which is reduced to clusters before the nickel or cobalt deposition process starts (this is the usual electroless deposition scenario). Then, on nickel or cobalt nuclei, the growth is autocatalytic. Coalescence of growing nuclei/clusters can yield a metal coating of the TMV, as seen in Figure 6. This coating is rather thick and not smooth, suggesting fast growth at few nucleation centers.

2.4. Electroless Deposition of Nickel and Cobalt in the Viral Channel

In another series of experiments the virions were dialyzed against water prior to activation and metallization, in order to remove the Na/K phosphate buffer. Again, without activation no metallization was obtained. We firstly deposited nickel from hypophosphite baths on activated TMV. TEM showed that only a small part of the virion rods exhibited large electron-dense clusters (nickel), i.e., clusters with diameters of 5–10 nm; they had even grown between the virions. The majority of virions appeared unchanged, while about a quarter were filled with up to 6 clusters, forming black spots inside the gray virion (see Fig. 7). Note that the clusters were located in the channel (compare with Fig. 2 for a uranyl-stained channel) at variable distances from the virion rod end. Furthermore, many clusters were not spherical, but elongated or rod-shaped with a diameter of ca. 3 nm (slightly less than the 4 nm channel diameter). Energy dispersive X-ray spectroscopy (EDX) proved that these clusters contained nickel. Figure 7 actually shows two head-to-tail arranged virus particles. This aggregation phenomenon was frequently observed; the slightly bent shape of the lower particle was also found quite often in single and aggregated particles.

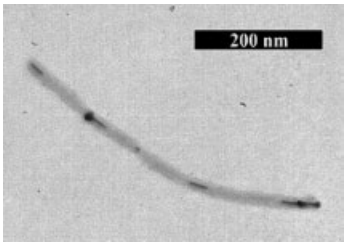

Figure 7. TEM image (200 kV) of two head-to-tail aggregated TMV particles after activation with Pd^{II} and contact with an electroless nickel bath (nickel-phosphinate). Small and also elongated electron-dense clusters are distributed inside the channel. EDX studies proved that the clusters are composed of nickel.

Experiments with nickel and cobalt baths containing the stronger reductant dimethylamine-borane (DMAB)[23] yielded similar results, i.e., the deposition rate was sufficiently fast, but still controllable at only pH 6–7 (for cobalt pH 7–8) and 25 °C. A pre-treatment of the virions with Pd^{II} or Pt^{II} was also necessary in this case. Here, the virions showed metal rods inside their channels (see Fig. 8), which in some cases reached lengths of 600 nm (in linear arrangements of virions).[18]

The key for understanding the surprising switching of selectivity in the presence or absence of phosphate is the Pd^{II} activa-

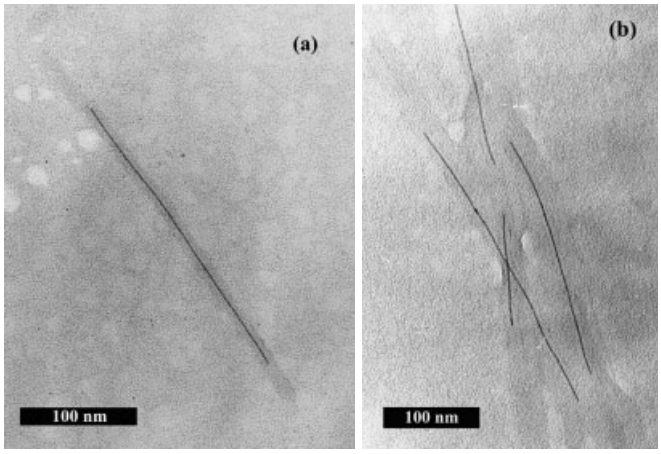

Figure 8. a) TEM (200 kV) image of a single virion containing a ca. 250 nm long nickel wire inside the central channel. Some unattached metal particles with diameters of 2–6 nm can be seen in the surrounding area. b) TEM (200 kV) image of several TMVs, arranged linearly and crossing each other, containing nickel wires of up to 300 nm length inside the inner channel.

tion (for Pt^{II} similar arguments apply). Under the conditions employed (much longer activation than for the palladium cluster coating in Sec. 2), there could be a concurrence between carboxylate and amine groups for palladium ions. The complexes of Pd^{II} with nitrogen-containing ligands are more thermodynamically stable, but kinetic effects can play a big role. Complexes of Pd^{II} with oxygen-containing compounds are kinetically stable.[28] Since oxygen-containing groups are easily accessible on the outer surface of TMV, complexes with Pd^{II} can form in addition to electrostatic bonding (see Sec. 2).

While the exterior surface of the protein coat (1 in Fig. 1) features alkyl chains, alcohol, carboxylate, and secondary amide groups, inside the channel, amine, primary amide, and guanidyl groups are found, in addition to the aforementioned groups, in the flexible loop of the protein (3 in Fig. 1). These groups can substitute Cl^- and H_2O in $PdCl_{4-n}(H_2O)_n^{n-2}$, hence we can assume the channel to contain Pd^{II}. This is likely to be the basis for the surprising confinement of the clusters inside the tube. In this context it should be mentioned that the narrow size of the channel should not be able to prevent the diffusion of small complexes such as $PdCl_4^{2-}$ within the channel (structure 4 in Fig. 1); even smaller openings can be filled by electroless deposition, as has been shown for carbon[32] and gold[26] nanotubes. In contrast to carbon nanotubes, the hydrophilicity of the protein loops should allow for a straightforward wetting of the channel by hydrophilic liquids, so the channel is supposed to be filled with water. When the ions are reduced and coalesce to clusters, they can act as activation centers for the electroless deposition of other metals such as nickel (note that, strictly speaking, we produce a nickel- and cobalt-rich NiP, NiB, or CoB phase that can be either crystalline or amorphous). We presume that the clusters are core–shell structured where the core comprises palladium and platinum, and the shell nickel and cobalt.

The complete absence of clusters on the exterior surface of TMV (1 in Fig. 1) may rely on the fact that even comparatively large gold or silver clusters can be stabilized by organic ligands, but palladium and platinum clusters cannot. The absence of phosphate means that upon contact with Ni^{II} or Co^{II} no precipitate (see Sec. 3) forms on the exterior surface. Additional destabilization can be caused by convection in the suspension or by forces acting on the metal clusters induced by gas (hydrogen) bubbles, which evolve during metallization (note that this is not the case when bound Pd^{II} is reduced). The metal particles detach from the exterior surface, while the metal clusters inside the central channel are encapsulated by the coat protein and thus can continue to grow. The result is a spatial selectivity in metallization that does not rely on a growth mechanism, but rather on secondary effects, like confinement in the hollow structure.

2.5. Self-Activated Electroless Deposition of Gold

The two step-method employed in the above-mentioned cases, activation and electroless deposition, can in some cases be replaced by a single-bath procedure ("self-activation"). For example, contact with a tetrachloroaurate-ascorbic acid bath[33] was expected to cover TMV firstly with gold atoms, then with gold clusters, and finally with a thicker deposit. However, only cluster formation was observed here; quite surprisingly, both short (15 min) and long (2 h) contact times lead to the same structure (see Fig. 9): After washing, dark spots with diameters in the nanometer range are found on the viral coat. Comparison with Figure 3, which does not exhibit such dark spots, indicates that the spots are indeed due to the presence of gold (organic material cannot produce a similar contrast). The channel region exhibits a dark gray line, which is not seen in the untreated virion (Fig. 3), but is seen with uranyl (Fig. 2). Note that the TEM result suggests staining of the outer surface (structure 1 in Fig. 1) and the inner channel (structure 4 in Fig. 1), similar to the uranyl treatment: Distinct spots could not be found. Due to the facile reduction of gold ions, we suspect that very small gold clusters are present (they can be nuclea-

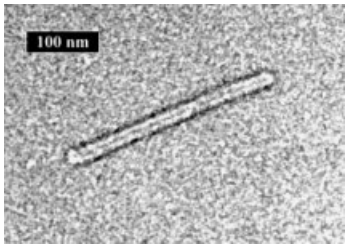

Figure 9. TEM image (200 kV) of TMV after contact with an electroless gold bath (tetrachloroaurate-ascorbic acid). Both the dark central channel and the very dark exterior surface indicate a dense coverage with gold (see text). The separation of the dark lines is ca. 15 nm, while the distance between the outer borders is ca. 20 nm.

ADVANCED FUNCTIONAL MATERIALS

tion centers for further metallization, see Sec. 6). In order to increase the metallization rate, the amount of gold ion ligand SCN^- (see Experimental) was lowered, which, on the other hand, led to a decreased stability of the bath. As expected, gold clusters started to form in solution immediately after preparing a bath with reduced SCN^- content,[33] even without adding the virus suspension. De-aeration of the bath with argon prior to the addition of $HAuCl_4$, as well as increased temperature and higher pH, decreased the stability of the bath further. Indeed, de-aeration often speeds up electroless depositions, since the reductants can no longer react with dissolved oxygen, and also temperature and a high pH value enhance the reaction rate.

Gold shows no large spatial selectivity. This is due to the chemistry of the gold bath: SCN^- substitutes the Cl^- ligands, and SO_3^{2-} reduces Au^{III} to Au^I. The resulting $Au(SCN)_2^-$ is stable in presence of SCN^-.[28] It can bind to amino acids[34] and proteins.[35] Subsequently the Au^I is reduced by ascorbic acid to metallic gold. The presumably strong preference for the only sulfur-containing group at Cys-27 should not play a role, since this amino acid is barely accessible. We suggest the following scenario: none of the potential ligands (–NHCO–, $–NH_2$, –COOH, –OH) can displace SCN^-, since this would normally require very soft ligands like Cys. Thus the complex binds electrostatically, in analogy to uranyl acetate. For the channel region we cannot find distinct clusters (see Fig. 9); however, due to the facile reduction of gold ions it is likely that very small clusters that are not resolved in our TEM images are produced. On the exterior viral surface, the fact that only small clusters are observed (small black spots) could mean that the amount of bound gold ions is so small that their coalescence upon reduction quickly consumes all gold atoms. Gold is now bound in the form of stable clusters, similar to gold clusters conjugated to antibodies available for immuno-gold labeling.[14] The separation of the dark lines in Fig. 9 (ca. 15 nm) indicates that the apparent staining cannot be exclusively negative, since in this case the metal would aggregate exclusively at the extreme outer surface of the virion, and the distance would be 18 nm. On the other hand, with an exclusive positive staining the distance between the outer borders of the dark coating would be 18 nm, which does not match our case either (ca. 23 nm). We propose a mix of positive and negative staining in this case.

2.6. Electroless Deposition of Nickel and Cobalt After Gold Activation

We employed the same procedure as was used for nickel and cobalt deposition after palladium and platinum activation, but used the gold-treated TMV described in Section 5 (see Fig. 9). As was already mentioned, deposition was only possible when the TMV was pre-treated (here with gold). Changes of pH and temperature had similar effects as in those reactions with palladium or platinum pre-treated TMV. The incubation times in the Ni^{II} and Co^{II} baths were longer than with the Pd^{II}- and Pt^{II}-pre-treated virion. TEM investigations showed that the majority of virions exhibited only those changes that are due to the gold treatment, i.e., the central channel and the surface had a much higher contrast than untreated TMV. However, when the hypophosphite-containing Ni^{II} bath was used, about a quarter of the virions showed additional cluster growth, which appeared to be exclusively limited to the virion surface. In no case did the clusters cover more than 30 % of the viral surface (Fig. 10). Figure 10b shows clusters not only at the sides of the virions, but also partly on top of the viral rod. From this we infer that no staining took place, rather a low-density coverage of the outer surface (for a high-density coverage (with palladium) see Fig. 5).

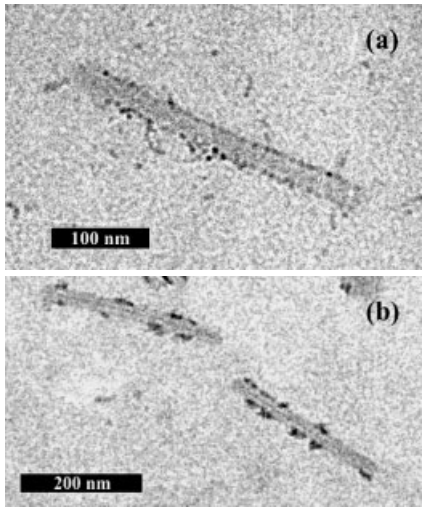

Figure 10. TEM images (200 kV) of TMV particles after activation with an electroless gold bath (tetrachloroaurate-ascorbic acid, see Fig. 9) and contact with an electroless nickel bath (nickel-phosphinate). Clusters are formed in the channel and on the exterior surface. a) TMV treated with this protocol (gold and nickel) is often not distinguishable from Figure 9 (gold only), but larger nickel clusters can be formed (b) (two virions). The width of the virions is ca. 18 nm.

When the gold-treated virions were immersed in a DMAB-containing Ni^{II}- or Co^{II}-bath, increased growth of metal at the exterior surface of the TMV could be observed (see Fig. 11). The results for both nickel and cobalt were similar. About 60 % of the virions contained metal after such a treatment, and the coverage of the exterior surface with metal reached 100 % in most cases.

Here, an increased stability of attached gold clusters to proteins comes into play. In contrast to palladium or platinum,

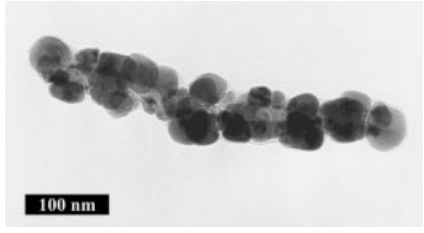

Figure 11. TEM (200 kV) of gold-pre-treated TMV metallized with cobalt from a DMAB-containing Co^{II}-bath. The exterior surface of the TMV is densely covered with cobalt.

small gold clusters can be stabilized by proteins very well, as was shown in Section 5, and as is known from immuno-gold labeling of proteins. The critical stage is probably the fast growth of cobalt or nickel—caused by the strong reductant DMAB—on the gold cluster. The high bonding strength of the nucleation center (gold cluster) to the coat protein hinders the detachment of the growing cluster, at least to a certain degree. When the metal clusters coalesce and form a sheath around the virion, attachment to the protein is secured mechanically.

2.7. Overview

The metallizations shown here are based on activations with either Pd^{II} (Pt^{II} behaves similarly) or Au^{III}. Any explanation has to be based on the possibilities of binding these metal ions to the virion. The precursors for virion metallization are metal ions in aqueous solution. The nature of the resulting bonds between virion and the metal ions will be the decisive factor for the spatially selective and stable attachment of the metal. As a general model we suggest that a metal ion binds electrostatically or via complex formation to the virion. TMV offers a multitude of charged groups and possible ligands for all of the metal ions employed, notably hydroxyl and carboxylate groups on its exterior protein surface (surface 1 in Fig. 1).[13] The RNA and the innermost protein loops are located surrounding the central channel (see Fig. 12). The loops (surface 3 in Fig. 1) comprise threonine and glutamine moieties, and they are flexible: They contain only very few hydrogen bonds, in contrast to the more rigid α-helical parts of the protein. Due to the flexibility of the loops, in addition to glutamine other amine-containing amino acids such as arginine may reach into the channel.[13] In contrast to oxygen-containing groups, amine groups are stronger ligands for noble metal ions such as Pd^{II} and Pt^{II}. However, the majority of the amino acids are not or hardly accessible, since they are situated inside the coat proteins where four adjacent α-helices provide a dense and rigid structure (2 in Fig. 1), and the strong metal ion ligands His and Met are not present. A very good example of the reduced accessibility is Cys-27, which should bind strongly to all metal ions employed, but is located deep inside the compact protein structure. In this respect it should also be noted that the large majority of functional groups on the outside of a single coat protein molecule (Fig. 12a) are not accessible, since they are situated at the interface between two proteins. Although in some cases, e.g., high pH or low Ca^{II} concentration,[7] the coat proteins can—reversibly—partially detach and thus allow diffusion inside each detached protein, we never observed an indication for this: Metal clusters were never located in the protein coat (position 2 in Fig. 1), but exclusively on the viral surfaces, i.e., either on the exterior coat or inside the central channel. However, the existence of very small clusters inside the protein layer, which are not easily detectable by TEM, cannot be ruled out. From these considerations, we can assume a slight preference for the inner channel since more amine groups are present. This explains the results for long Pd^{II} and Pt^{II} activation times,

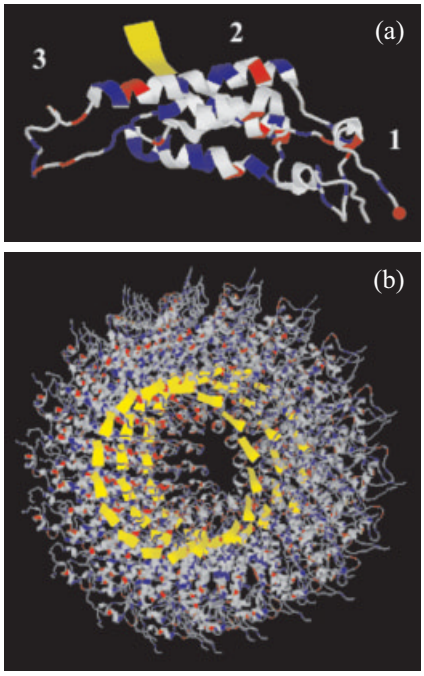

Figure 12. Models of TMV components of a rod section, generated with data from ref. [11] (file "2tmv", strain vulgare). The protein backbone is shown as a line; α-helices and the RNA (yellow) are shown as ribbons. The carboxylate side chain molecules are colored red, the amine side chain molecules blue. a) Model of a single coat protein subunit. The flexible loop (left, surface 3 in Fig. 1) points inside the channel, the middle part (2) comprises four rigid α-helices (ribbons), and only the very right part (1) forms the exterior viral surface (the four last amino acids Gly(or Ser)-Pro-Ala-Thr-COOH with the terminal carboxylate group are represented by a red dot). Here we find OH and COOH groups, but also several alkyl side groups. b) Model of 49 protein subunits, corresponding to three of ca. 130 helical turns (the last four amino acids at the COOH terminus are omitted); compare to Figure 1.

namely the formation of very small clusters inside the channel, on which nickel and cobalt can grow to clusters and wires. Probably more important is that larger clusters cannot remain attached to the outer surface, since neither complex formation nor electrostatic interactions come into play.

The presence of phosphate changes the scenario completely, since this anion attaches to the positively charged outer viral surface. It can then promote the selective attachment of Ni^{II} and Co^{II} in the electroless deposition baths, but Pd^{II} and Pt^{II} must still be present. Electroless deposition now yields larger clusters of nickel and cobalt exclusively on the outer viral surface. Here the attachment is purely mechanical, and for this reason the clusters have to grow fast and coalesce to coat the virion completely. For gold activation, similar arguments are valid, with some exceptions: First, Au^{I} is present as $Au(SCN)_2^-$, which should bind exclusively by electrostatic interactions. Second, we already employ an electroless deposition bath for the activation. The resulting gold clusters can remain attached to the various surfaces of the virion. This explains the observed structure with gold inside the channel and on the outer viral surface. Third, we tuned the bath composition to a very small

ADVANCED FUNCTIONAL MATERIALS

Table 1. Overview of the results of metallization of TMV. The column "buffer" indicates, whether the virus suspension was dialyzed prior to metallization (no buffer present) or not (phosphate buffer present). The column "in/out" indicates whether the metal deposition took place inside the inner channel (in., 4 in Fig. 1) of the virion or at the outer surface (out., 1 in Fig. 1).

deposited metal	activation	reductant	buffer	in./out.
Ag (ref.15)	no	HCHO; light	yes	clusters out. (staining)
Pd	no	NaH_2PO_2	no	clusters out.
Pd	no	DMAB	no	clusters out.
Au	no	ascorbic acid	no	in. and out. (staining)
Ni	Pd(II); Pt(II)	NaH_2PO_2	no	clusters/wires in.
Ni	Pd(II); Pt(II)	DMAB	no	wires in.
Ni	Pd(II); Pt(II)	DMAB	yes	coating out.
Ni	Au(III)	DMAB	no	coating out.
Co	Pd(II); Pt(II)	NaH_2PO_2	no	no metallization
Co	Pd(II); Pt(II)	DMAB	no	wires in.
Co	Pd(II); Pt(II)	DMAB	yes	coating out.
Co	Au(III)	DMAB	no	coating out.
Ru	Pd(II); Pt(II)	NaH_2PO_2 or DMAB	no	in. and out. (staining)
Ru	no	NaH_2PO_2 or DMAB	no	in. and out. (staining)

deposition rate, counteracting further growth of the gold. Again, electroless deposition of nickel and cobalt on the gold clusters yields larger clusters on the outer viral surface, while the channel should remain filled with small gold clusters.

3. Conclusions

We showed that metal clusters can be deposited selectively either on the exterior surface or in the central channel (or both) of a plant virus nanotube. A range of different tobacco mosaic virus (TMV)–metal composites were prepared from virus suspensions in water or in phosphate buffer by contact with Pd^{II}, Pt^{II}, and Au^{III} solutions and subsequent electroless deposition of nickel and cobalt. We propose specific ligand–metal ion interactions in which the ligand is a functional group of the virion structure. A proper choice of metal ion, pH, and duration of treatment leads to the preference of certain groups. Due to the nature of the virion, these groups can be concentrated on the exterior surface or in the channel (or both). In this way, metal ions and their reduction products, clusters, can be placed on selected regions of the viral nanotube. We coated these clusters with nickel and cobalt by electroless deposition. The exterior surface can be covered by individual palladium, platinum and gold clusters of less than 3 nm diameter, or with a sheath of interpenetrating nickel and cobalt clusters, each of more than 50 nm diameter. In the absence of phosphate buffer, the 4 nm wide channel can be filled with nickel and cobalt clusters which are often rod-shaped with a diameter of about 3 nm, while faster electroless deposition yields 3 nm wide nickel and cobalt wires of several 100 nm length.

4. Experimental

Water was purified with a Millipore Milli-Q or a Barnstead Nanopure apparatus to 18.2 MΩ cm. A suspension of TMV *vulgare* was employed to mechanically infect *Nicotiana tabacum* cv. Samsun nn plants. 4 weeks post-inoculation, systemically infected leaves were harvested and stored at –20 °C. We also infected the plants with plasmid DNA that comprised the code for the movement and coat protein of the TMV genome as well for the replicase. In this case the coat protein differed very slightly from *vulgare*: Ser-155 replaces Gly-155. Two methods were employed to isolate the virus, including centrifugation in CsCl or sucrose gradients, yielding 10 mg mL^{-1} TMV suspensions in water. They were stored at 4 °C. In some cases we replaced water with Na_2HPO_4/KH_2PO_4 buffer (pH 7, "Na/K buffer"). We found considerable degradation (particles < 300 nm long) after several months of storage at 4 °C in water, but only for the *vulgare* strain. In some cases (see Results) the TMV suspensions were dialyzed against pure water using Slide-A-Lyzer 10000 MWCO caps (KMF, Lohmar).

Copper or nickel grids (300 or 400 mesh) were washed with 0.1 M HCl (Merck), 99.8 % ethanol (Roth), and acetone (Roth), each for 10 s, and coated with pioloform. A thin layer of carbon (8–10 nm) was evaporated at 2×10^{-5} mbar on top. Immediately prior to use, the grids were dipped into ethanol (Roth Rotipuran > 99.8 %) and dried. 20 μL of TMV suspension was placed on top of a grid for 1 min. The solution was removed by use of filter paper.

For negative staining, 20 μL of a 0.2–0.5 mg mL^{-1} TMV suspension was placed on a TEM grid for 30 s, then washed with water. 2 % $UO_2(CH_3COO)_2{\cdot}2H_2O$ (Merck) and 0.5 mg mL^{-1} bacitracin (Sigma) were mixed 1:1 and centrifuged for 5 min at 14 000 g. 100 μL of this solution was placed on the grid for 1 min. Surplus liquid was removed with paper.

For the Pd^{II} and Pt^{II} activation treatments, 100 μL of a 0.2 mg mL^{-1} TMV suspension in water were mixed with the same amount of a freshly prepared 3 mM Na_2PdCl_4 (Aldrich 99.998 %) or $Na_2PtCl_4{\cdot}xH_2O$ (Aldrich) solution in water, pH-adjusted with HCl to between 3 and 5.5. In most cases a pH 5.5 solution was used (see also ref. [23]). After 2–15 min., the suspension was centrifuged for 4 min at 14 000 g, producing a pale brown pellet. The supernatant was removed and the pellet washed twice with water by re-suspension and repeated centrifugation. Alternatively, the Pd^{II}- or Pt^{II}-treated TMV suspension was dialyzed against water as detailed above.

To obtain palladium clusters, NaH_2PO_2 (p.a., Fluka) was added to the palladium solution to 30 mM. The solution was mixed with the same amount of 0.1 mg mL^{-1} TMV suspension, and after a reaction time of ca. 20 min. placed on a TEM grid for 30 s. The liquid was afterwards removed with filter paper.

For the electroless deposition of gold, an Au^{III} bath slightly modified from ref. [33] was applied. The bath contained 0.03 M Na_2SO_3 (Fluka), 0.1 M NaSCN (Aldrich), 0.1 M L-(+)-ascorbic acid (Aldrich) and 0.01 M $HAuCl_4{\cdot}3H_2O$ (Aldrich), adjusted to pH 6 with 10 % HCl. The (pure) TMV suspension was mixed with an equal volume of the gold bath and heated to 60 °C for 15–90 min.

Pd^{II}-pre-treated TMV suspension was metallized with nickel by mixing the suspension with an equal volume of a solution containing 0.1 M $NiCl_2{\cdot}6H_2O$ (Sigma), 0.43 M $NaH_2PO_2{\cdot}H_2O$ (Fluka p.a.), 0.3 M $Na_2B_4O_7$ (Aldrich) and 0.03 M glycine (Fluka), adjusted to pH 9 using 1 M NaOH [36]. In order to stop the metallization (after 1–2 min), the solution was diluted with water up to 10-fold.

Metallization of palladium- and platinum-pre-treated TMV with dimethylamine-borane (DMAB)-containing Ni^{II} or Co^{II} baths was carried out according to ref. [23]. The nickel bath was freshly prepared from 0.18 M $Ni(CH_3COO)_2{\cdot}4H_2O$ (p.a., Fluka), 0.28 M lactic acid (85 % in water, Fluka) and 34 mM DMAB (p.a. Aldrich) in water. The pH was adjusted to 6–7 with 1 M NaOH solution. The palladium- or platinum-pre-treated TMV suspension was mixed after washing with the same amount of the Ni^{II}-containing solution. After gas evolution started, 30 μL of the solution was placed on a TEM grid for 30 s and afterwards removed with filter paper. The same procedure was applied for the metallization with cobalt. The only difference was the composi-

tion of the bath: 0.16 M $CoSO_4 \cdot H_2O$ (p.a., Fluka), 0.15 M sodium succinate (p.a., Fluka) and 7 mM DMAB (p.a., Aldrich) in water. The bath was adjusted to pH 7–8 with 1 M NaOH [23].

Deposition of nickel or cobalt was tested with the same Ni^{II} or Co^{II} baths, but without Pd^{II}, Pt^{II}, or Au^{III} pre-treatment of the TMV. The same volumes of Ni^{II}- and Co^{II}-containing solutions were added to the TMV suspensions. After several hours, no gas evolution could be observed and TEM micrographs did not show changes in contrast, as compared to the native virion.

Au^{III}-pre-treated TMV suspension was metallized with nickel by electroless deposition of gold (see above), then washing and treating the virus suspension with either the $NaH_2PO_2 \cdot H_2O$-containing Ni^{II} bath for 10–20 min, or with a DMAB-containing Ni^{II}- or Co^{II} bath for 5–15 min. The solution was then diluted with water up to 10-fold, and 30 μL of the solution was placed on a grid for 30 s and afterwards removed with filter paper.

For transmission electron microscopy (TEM) measurements a Zeiss EM10 operating at 60 kV, a Philips CM200 operating at 200 kV, and a JEOL-4000 FX operating at 400 kV were used.

Received: March 14, 2003
Final version: November 6, 2003

[1] C. P. Collier, E. W. Wong, M. Belohradský, F. M. Raymo, J. F. Stoddart, P. J. Kuekes, R. S. Williams, J. R. Heath, *Science* **1999**, *285*, 391.
[2] T. S. Ahmadi, Z. L. Wang, T. C. Green, A. Henglein, M. A. El-Sayed, *Science* **1996**, *272*, 1924.
[3] A. P. Alivisatos, *Science* **1996**, *271*, 933.
[4] H. Frey, K. Lorenz, C. Lach, *Chem. Unserer Zeit* **1996**, *30*, 75.
[5] R. M. Crooks, M. Zhao, L. Sun, V. Chechik, L. K. Yeung, *Acc. Chem Res.* **2001**, *34*, 181.
[6] T. M. A. Wilson, R. N. Perham, *Virology* **1985**, *140*, 21.
[7] G. Stubbs, *Philos. Trans. R. Soc. London, Ser. B* **1999**, *354*, 551.
[8] M. Demir, M. H. B. Stowell, *Nanotechnology* **2002**, *13*, 541.
[9] T. Douglas, M. Young, *Nature* **1998**, *393*, 152.
[10] Q. Wang, T. Lin, L. Tang, J. E. Johnson, M. G. Finn, *Angew. Chem. Int. Ed.* **2002**, *41*, 459.
[11] a) http://pqs.ebi.ac.uk/pqs-bin/macmol.pl?filename=2tmv. b) K. Henrick, J. M. Thornton, *Trends Biochem. Sci.* **1998**, *23*, 358. c) R. Pattanayek, G. Stubbs, *J. Mol. Biol.* **1992**, *228*, 516. d) K. Namba, R. Pattanayek, G. Stubbs, *J. Mol. Biol.* **1989**, *208*, 307.
[12] A. Klug, *Phil. Trans. R. Soc. London, Ser. B* **1999**, *354*, 531.
[13] W. Shenton, T. Douglas, M. Young, G. Stubbs, S. Mann, *Adv. Mater.* **1999**, *11*, 253.
[14] M. Bendahmane, M. Koo, E. Karrer, R. N. Beachy, *J. Mol. Biol.* **1999**, *290*, 9.
[15] M. Knez, M. Sumser, A. M. Bittner, C. Wege, H. Jeske, S. Kooi, M. Burghard, K. Kern, *J. Electroanal. Chem.* **2002**, *522*, 70.
[16] E. Dujardin, C. Peet, G. Stubbs, J. N. Culver, S. Mann, *Nano Lett.* **2003**, *3*, 413.
[17] a) G. A. Kausche, H. Ruska, *Kolloid-Z.* **1939**, *89*, 21. b) G. A. Kausche, *Biol. Zentralbl.* **1940**, *60*, 179.
[18] M. Knez, A. M. Bittner, F. Boes, C. Wege, H. Jeske, E. Maiß, K. Kern, *Nano Lett.* **2003**, *3*, 1079.
[19] a) M. Zaitlin, *AAB Descriptions of Plant Viruses* **2000**, *370*, 8. b) R. N. Perham, T. M. A. Wilson, *Virology* **1978**, *84*, 293.
[20] M. Knez, M. P. Sumser, A. M. Bittner, C. Wege, H. Jeske, D. M. P. Hoffmann, K. Kuhnke, K. Kern, *Langmuir*, DOI: 10.1021/la0354250.
[21] J. Richter, M. Mertig, W. Pompe, I. Mönch, H. K. Schackert, *Appl. Phys. Lett.* **2001**, *78*, 536.
[22] E. Braun, Y. Eichen, U. Sivan, G. Ben-Yoseph, *Nature* **1998**, *391*, 775.
[23] M. Mertig, R. Kirsch, W. Pompe, *Appl. Phys.* **1998**, *A66*, S723.
[24] M. Reches, E. Gazit, *Science* **2003**, *300*, 625.
[25] T. Scheibel, R. Parthasarathy, G. Sawicki, X.-M. Lin, H. Jaeger, S. L. Lindquist, *Proc. Natl. Acad. Sci. USA* **2003**, *100*, 4527.
[26] K. B. Jirage, J. C. Hulteen, C. R. Martin, *Anal. Chem.* **1999**, *71*, 4913.
[27] M. Pourbaix, in *Atlas of Electrochemical Equilibria*, National Association of Corrosion Engineering, Houston, TA **1974**.
[28] *Gmelins Handbuch der Anorganischen Chemie*, 1st ed., Verlag Chemie, Weinheim **1954**.
[29] Y. S. Chang, M. L. Chou, *J. Appl. Phys.* **1991**, *69*, 7848.
[30] M. Ramani, B. S. Haran, R. E. White, B. N. Popov, *J. Electrochem. Soc.* **2001**, *148*, A374.
[31] H. Kind, A. M. Bittner, O. Cavalleri, K. Kern, T. Greber, *J. Phys. Chem. B* **1998**, *102*, 7582.
[32] J. Li, M. Moskovits, T. L. Haslett, *Chem. Mater.* **1998**, *10*, 1963.
[33] Y. Okinaka, M. Hoshino, *Gold Bull.* **1998**, *31*, 3.
[34] J. Pouradier, *Chimia* **1974**, *24*, 374.
[35] J. Pouradier, A. M. Mailliet, B. Cerisy, *J. Chim. Phys. Phys.-Chim. Biol.* **1966**, *63*, 469.
[36] Y. V. Prusov, V. F. Makarov, V. N. Flerov, *Izv. VUZOV Khim. Khim. Tekh.* **1992**, *35*, 3.

